

Volumetric subtraction angiography for image-guided therapy

D.E. Hyde^{*1,3}, A.J. Fox^{2,3}, T.M. Peters^{1,3}, S.P. Lownie^{2,3}, D.F. Habets^{1,3}, D.W. Holdsworth^{**1,3}

¹John P. Robarts Research Institute; ²London Health Sciences Centre;

³University of Western Ontario, London, Ontario, Canada

ABSTRACT

Our goal is to improve the visualization of the intracranial vasculature during interventional procedures where radiographically dense objects would normally hinder clinical assessment. We describe our technique of Volumetric Subtraction Angiography (VSA), which removes bone, metal objects, and associated artifacts from the 3-D contrast-enhanced image of the patient's vasculature. This work utilizes a prototype Computed Rotational Angiography (CRA) system that uses a C-arm mounted x-ray image intensifier to acquire 2-D projections of the vasculature. A modified cone-beam computed tomography (CT) algorithm is then used to reconstruct a 3-D image with isotropic voxels. Two volumes of data are acquired, and the anatomical mask is volumetrically subtracted (voxel-by-voxel) from the intra-arterial, contrast-enhanced image, producing a 3-D angiogram.

Keywords: volumetric subtraction angiography, image-guided therapy, computed tomography, computed rotational angiography, 3-D angiography, image registration, intra-arterial, cerebral-vasculature

1. INTRODUCTION

Cerebral aneurysms are typically diagnosed using high-resolution digital-subtraction angiography (DSA) images, acquired at a variety of viewing angles. These images are used to determine the most appropriate therapy, either surgical clipping or endovascular occlusion.^{1,2} Factors influencing the choice of treatment include the size and shape of the aneurysm,^{3,4} the size of the aneurysmal neck,⁵ and the relationship of the neck to adjacent arterial branches.

Currently, guidance during catheter manipulation is provided almost exclusively by x-ray imaging, due to the fundamental advantages in temporal and spatial resolution provided by DSA systems.⁶ Conventional DSAs are produced by subtracting a 2-D anatomical-mask projection from a 2-D contrast-enhanced projection. If these projections contain a dense, radiographically opaque, metal object, it may appear as a region of zero intensity. Consequently, the object's shadow on the detector does not contain any information, resulting in a condition known as under-ranging. Vessels overlapping this region are completely obscured, and many acquisition angles are often required to examine the clinically relevant vasculature. During endovascular therapy, this limitation can make it difficult to obtain complete packing of an aneurysm with coils, avoiding a residual neck.^{7,8,9} It may also be difficult to bridge the neck of the aneurysm without occluding the parent vessel,¹⁰ in which case 3-D visualization could also assist with balloon remodeling or stent implantation.

Angiographic visualization during neurosurgery is also limited, although it can be the key to the success of the procedure.^{11,12} For example, studies have indicated improper placement of aneurysm clips in about 30% of cases.^{13,14} Thus, when angiography is available during neurosurgery, such misplacements can be corrected before complications arise. Although image-guidance has had a significant impact on neurovascular therapy, there is a serious limitation in the visualization of the small perforating arteries that must be preserved to avoid stroke and serious handicaps.^{15,16} At present, no existing imaging technique can be used to visualize these small vessels (<0.3 mm) in 3-D.

A promising approach to providing 3-D image guidance during interventional neurovascular therapy and surgery is to modify existing C-arm based DSA systems to perform conebeam 3-D computed tomography (CT). We have called this

*dhyde@irus.ri.on.ca, phone (519)685-8300 x34324, fax (519)663-3900, Imaging Research Laboratories, Robarts Research Institute, 100 Perth Dr., P.O. Box 5015, London, ON, Canada, N6A 5K8.

**dholdsw@irus.ri.on.ca, phone (519)685-8300 x34154, fax (519)663-3900, Imaging Research Laboratories, Robarts Research Institute, 100 Perth Dr., P.O. Box 5015, London, ON, Canada, N6A 5K8.

technique computed rotational angiography (CRA),¹⁷ to avoid confusion with CT angiography (CTA) performed by helical CT scanners, and to distinguish it from rotational angiography performed without CT reconstruction. We have shown that conventional digital-radiographic systems can also be used to collect projections from many angles around the patient, resulting in a 3-D CT reconstruction.¹⁷ This required the development of techniques to calibrate and correct geometric distortions in the XRII at arbitrary acquisition angles,¹⁸ to characterize and correct non-ideal motions of the C-arm during its trajectory around the object of interest,¹⁹ as well as the development of algorithms for rapid cone-beam reconstruction of volumes as large as 400^3 voxels.

CRA generates 3-D reconstructions with inherently isotropic voxels. This minimizes the partial volume effects that are common in other modalities with an axial slice thickness greater than the in-plane resolution. Reducing this effect is of particular importance when imaging radiographically dense metal and iodinated vascular contrast agents.²⁰ Although computationally intensive, CRA images are ideally suited to 3-D registration and subtraction procedures, since image blurring from trilinear interpolation is reduced with high-resolution isotropic voxels. CRA provides high-contrast, anatomical landmarks that are ideal for image fusion with other modalities (figure 1). For example, a high-density bone in a CRA can be mapped to the corresponding signal void in an MRI (Magnetic Resonance Image).

This paper describes our prototype CRA system, acquisition parameters, and volumetric subtraction angiography (VSA), which removes the bone and metal structures from our 3-D angiograms. Results from our preliminary patient study are presented.

2. METHODS

2.1 CRA system

This work uses a prototype CRA system (Multistar, Siemens Medical Systems, Erlangen) consisting of a conventional clinical C-arm with a 40 cm x-ray image intensifier (XRII) and a 1.5 MHU tube (see figure 2). This system has been modified to allow rotation at 45° s^{-1} , while acquiring 30 frames s^{-1} .

A typical CRA image is obtained with a 28 cm field of view (FOV), acquiring 130 exposures (90 kVp, 250 mA, 5 ms) over 4.4 s, during a 6 s selective intra-arterial contrast injection. An iodinated contrast agent solution (contrast-to-saline ratio of 2:1) is used for both CRA and DSA, permitting the acquisition of both modalities for direct comparison. An intra-arterial injection rate of 3 to 4 ml/s is used for CRA. Digital images are transferred to a Unix network for cone-beam CT reconstruction.

2.2 3-D Visualization

Our images are viewed on SGI (Indy) and DEC (Alpha) Unix-based workstations. Maximum intensity projections (MIPs) and digitally reconstructed radiograms (DRRs) of the 3-D volume are produced with our own software, utilizing VTK (Visualization Toolkit, Kitware Inc, Clifton Park NY). These perspective renderings are created using trilinear interpolation and voxel driven algorithms. Volume rendering is performed in Voxel View, Version 2.5 (Vital Images, Plymouth, Minnesota).



Figure 1: Axial slice from a contrast-enhanced CRA, illustrating the high contrast anatomical landmarks.

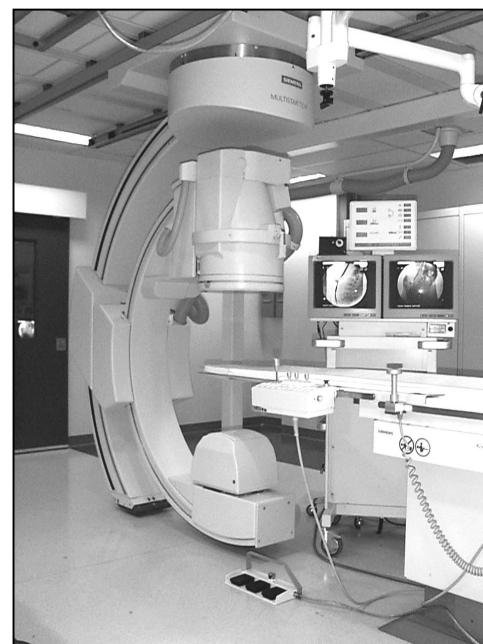


Figure 2: Prototype CRA system.

2.3 Volumetric subtraction

Specialized cone-beam computed tomography (CT) software is used to reconstruct a 3-D image. A VSA is then constructed by the voxel-by-voxel subtraction of an anatomical-mask volume from a contrast-enhanced volume. This approach eliminates bone and metal structures so that only the patient's vasculature is present in the final image.

A conventional 2-D x-ray projection (figure 3a) is similar to a maximum intensity projection (MIP) of a CRA, with opaque objects obscuring the underlying vasculature. In contrast, while the DSA still contains completely obscured regions (figure 3b), a MIP of a VSA does not (figure 3c). Since the CRA is acquired at multiple viewing angles, sampling the entire 3-D space, it produces an accurate representation of the entire volume and avoids the complete under-ranging normally associated with dense objects. Thus, upon volumetric subtraction of the bone and metal objects, the underlying vasculature is retained, and the entire vasculature can be viewed from virtually any perspective. This can provide unobscured visualization of the clinically relevant vasculature, such as the parent artery and aneurysm neck.

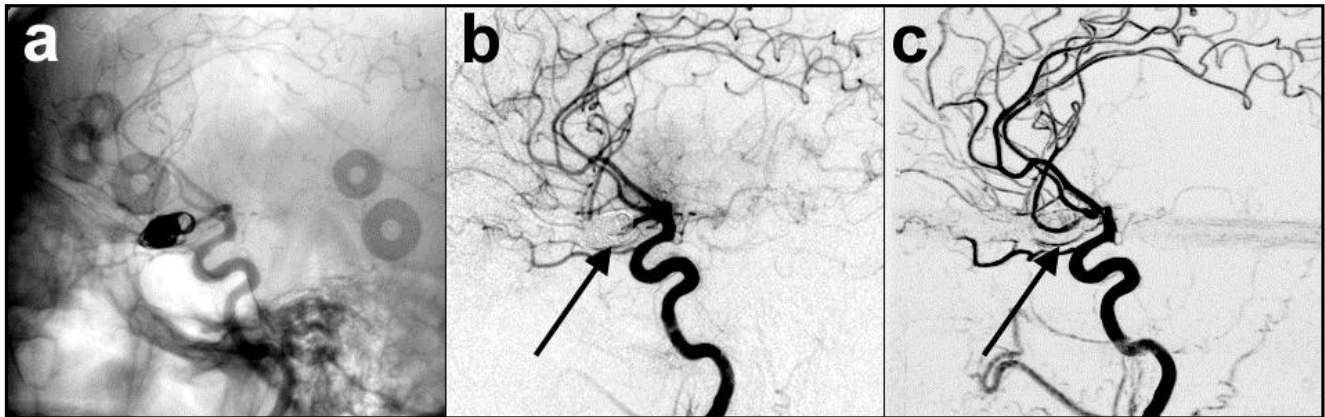


Figure 3: a) Conventional 2-D x-ray projection of the contrast-enhanced cerebral vasculature (follow-up study). b) The corresponding DSA illustrates the information void where the coils have been subtracted (arrow). c) The MIP of the VSA reveals the underlying vasculature upon volumetric subtraction of the coils.

2.4 Preliminary patient study

We have scanned 16 patients with cerebral aneurysms, 3 were untreated, 5 were clipped, 7 were coiled, and one was clipped and coiled. Some patients received more than one selective intra-arterial injection, thus a total of 21 VSAs were collected. In all cases, conventional digital subtraction angiography (DSA) was also performed, allowing direct comparison of the DSA, CRA and VSA images. These patients were either imaged during treatment planning or follow-up, and were all unanaesthetized. This represents the most difficult condition, as significant patient motion is possible.

2.5 Volumetric registration

Subtraction artifacts have been significant when previously treated (clipped/coiled) patients, who were not anaesthetized, have moved between the two scans. In these cases, artifacts may be reduced or eliminated by re-registration of the mask volume. This is analogous to the conventional 2-D DSA pixel shift. Unfortunately, simple translation of the 2-D projections (prior to backprojection) requires equivalent acquisition angles, and does not allow correction for patient motion between scans. Consequently, the entire volume must be translated and rotated in all 3 planes. This has been performed by manual selection of homologous points in the reconstructed volumes. A transformation matrix is then determined (using 3 rotation and 3 translation parameters), and the mask is trilinearly interpolated so that it registers with the contrast-enhanced scan, prior to volumetric subtraction. Thus by using true volumetric subtraction, we can correct for any rigid-body translation or rotation between the contrast-enhanced and anatomical-mask acquisitions. This could potentially allow repeated use of an anatomical mask (even with patient repositioning), thereby reducing the radiation dose to the patient.

3. RESULTS

3.1 3-D visualization

The CRA images acquired during our *in vivo* study exhibit higher contrast and spatial resolution than any other 3-D angiographic technique available, but they still do not have a sufficient signal-to-noise ratio (SNR) to visualize the smallest perforating vessels in the cerebral vasculature. Nonetheless, some of these patients have already benefited from the improved perception of complex geometries during treatment planning. A study with a complex vascular arrangement is illustrated in Figure 4a, which is a MIP of a giant basilar trunk aneurysm at a fenestration (lateral view). Figure 4b is a posterior-anterior volume rendered view of the same giant basilar trunk aneurysm at a fenestration. It would be difficult to surgically clip this aneurysm without obstructing the surrounding vessels, and thus it was successfully treated endovascularly, with detachable coils.

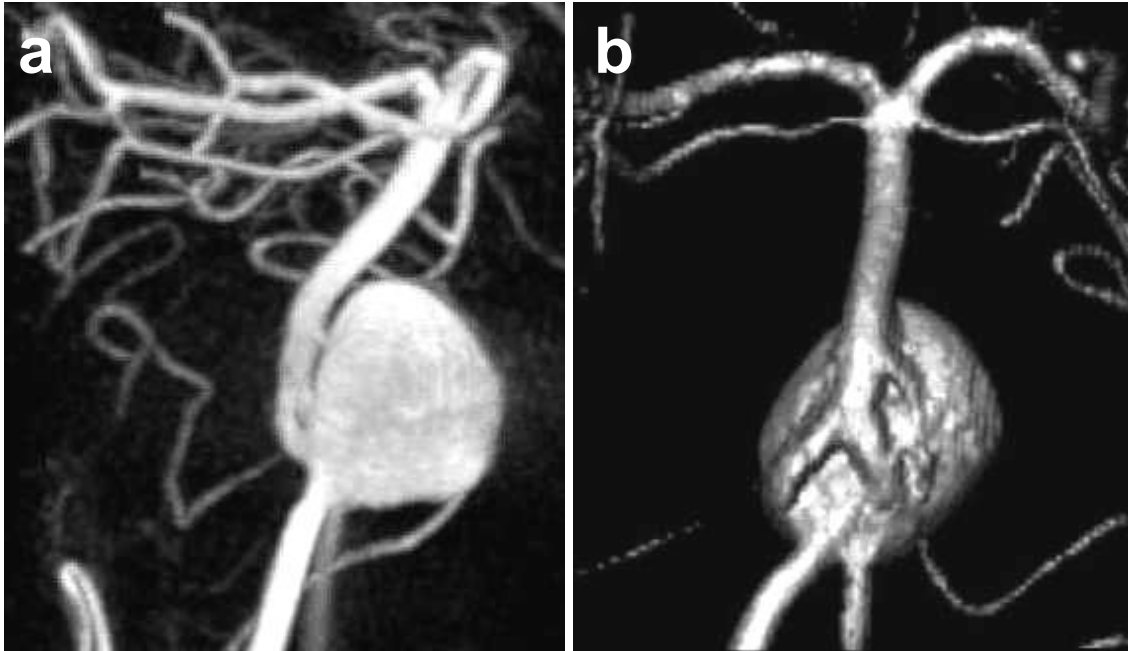


Figure 4: (a) Maximum intensity projection (MIP) of a giant basilar trunk aneurysm at a fenestration (lateral view). (b) Posterior-anterior volume rendered view of the same giant basilar trunk aneurysm at a fenestration.

3.2 Volumetric Subtraction

Follow-up VSAs have provided superior visualization of the patient's vasculature, clearly discerning the parent vessel and residual aneurysm near clips and coils. Figure 5a is a maximum intensity projection (MIP) from a typical CRA of a basilar tip aneurysm that has been filled with platinum coils. Figure 5b is the corresponding MIP from the VSA of the same basilar tip aneurysm. The coils have been subtracted, allowing unobstructed examination of the aneurysm neck and parent artery. In this case, the patient remained stationary between the anatomical-mask and contrast-enhanced acquisitions, so volumetric registration was not required.

3.3 Volumetric registration

In some patients, motion between the anatomical-mask and contrast-enhanced scans produced residual subtraction artifacts in the VSA, most notably in the follow-up scans containing high-contrast metal clips or coils. Figure 5c is a MIP from a CRA of a posterior communicating artery aneurysm that was previously clipped. Figure 5d is the corresponding MIP from the VSA of the same patient, note the residual clip artifact due to patient motion.

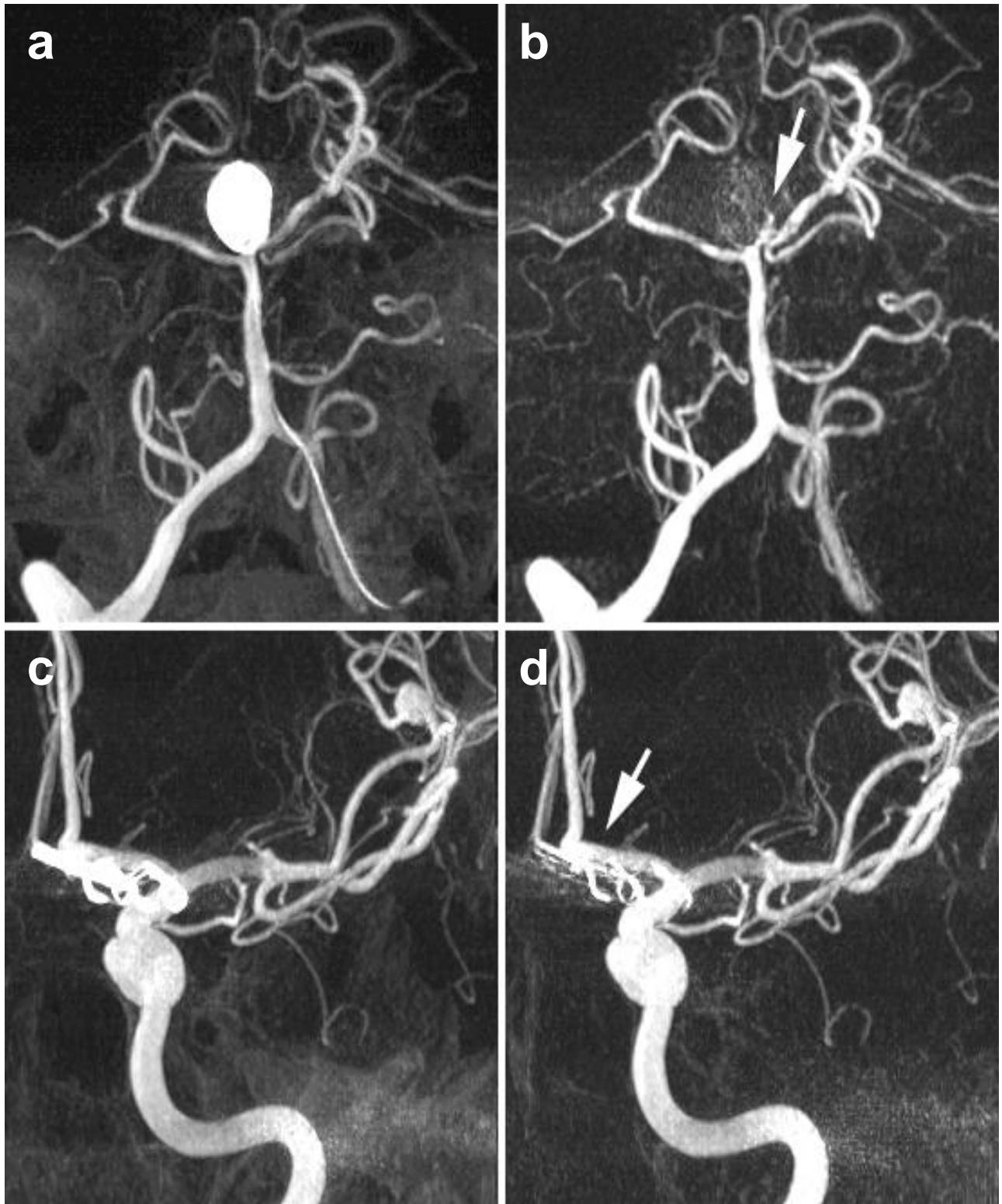


Figure 5: (a) MIP from a CRA of a basilar tip aneurysm filled with platinum coils (follow-up study). (b) MIP from the VSA of the same basilar tip aneurysm. The coils have been subtracted (arrow), allowing unobstructed examination of the aneurysm neck and parent artery. (c) MIP from a CRA of a posterior communicating artery aneurysm that was previously clipped. (d) MIP from the VSA of the same patient, note the residual clip artifact due to patient motion.

Figure 6a is an axial slice from a CRA, illustrating the high-contrast metal clips. Figure 6b is an axial slice from a VSA image, illustrating patient motion. Residual subtraction artifacts associated with the clips and sinuses, are shown in Figure 6b. Homologous points (anatomical landmarks as well as the metal clip) were manually selected in the anatomical-mask and contrast-enhanced volumes. A rigid-body transform (3 translations and 3 rotations) and trilinear interpolation were then used to register the anatomical mask to the contrasted volume. This registration, prior to subtraction, has significantly reduced the motion artifacts in the VSA (figure 6c). The corresponding MIPs are shown in figures 7. The motion artifact has been significantly reduced, but sub-voxel mis-registration of the high-contrast metal clips has left some residual partial-volume artifact.

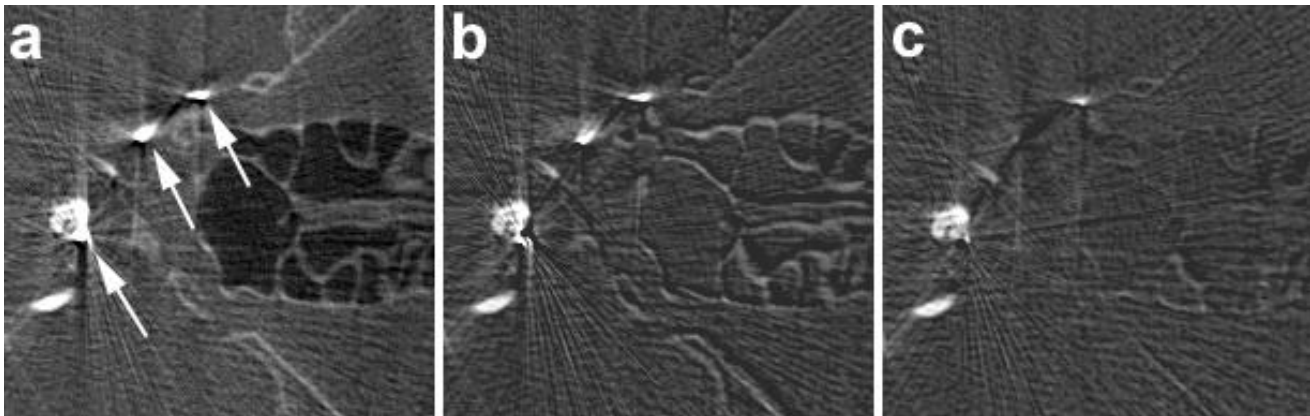


Figure 6: a) Axial slice from a CRA; note the high-contrast metal clips (arrows). b) Axial slice from a VSA. This illustrates the residual subtraction artifacts associated with the clips and sinuses. c) Manual registration of the mask volume, prior to subtraction, has significantly reduced these high-contrast motion artifacts.

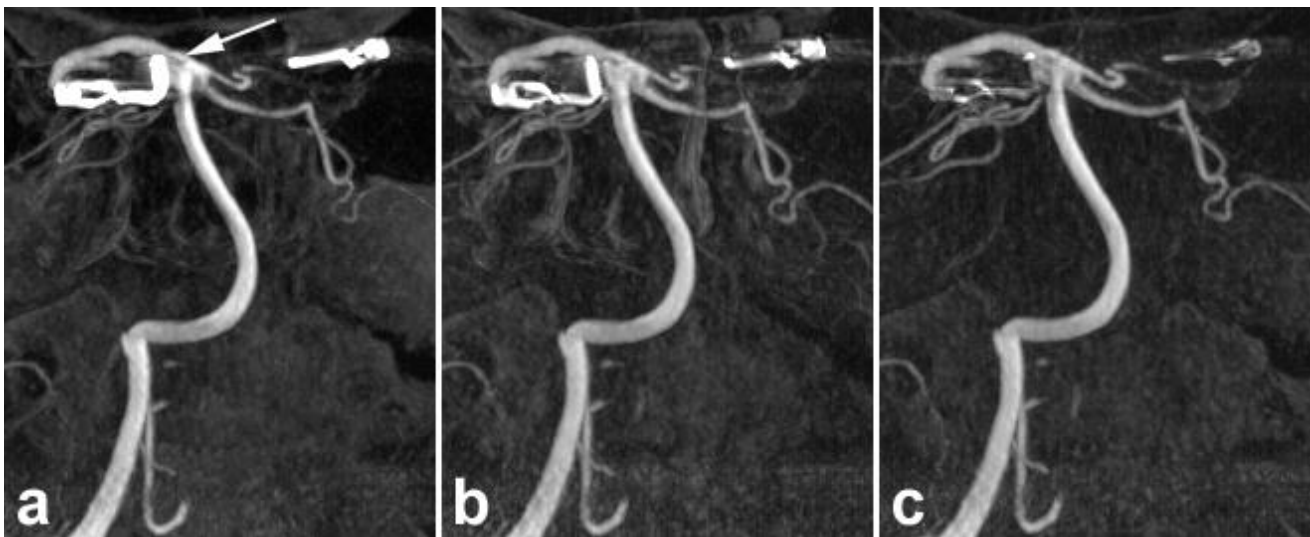


Figure 7: a) MIP of a CRA, showing how a clip may obscure visualization of the parent artery (arrow). b) MIP of mis-registered VSA, illustrating residual clip artifacts. c) MIP of a VSA, after manual volumetric registration, illustrating the reduction of the residual clip artifact. Note the improved visualization of small vessels in c.

4. DISCUSSION

Volumetric subtraction angiography is advantageous over conventional DSA. It provides unobstructed visualization of the vasculature near radiographically dense objects, which are common in interventional neurovascular therapies. It allows MIP views from any desired angle, optimizing diagnosis and treatment procedures. Finally, volume renderings can provide insight on intricate 3-D vessel configurations.

Volumetric registration has been useful in correcting patient motion during scans of patients who were not anaesthetized. While only four points are required to describe a volume, it was necessary to establish at least ten homologous points to achieve a sub-voxel precision of the registration. In most cases this resulted in the alignment of any clips/coils, improving the volumetrically subtracted angiogram. It should be noted that even a partial volume artifact (from a sub-voxel mis-registration of a high-contrast object) can produce a significant residual in a MIP.

Anatomical landmarks in the patient's skull are readily identified (figure 1), but this process is laborious. We are currently investigating automated registration techniques using software developed in the MINC environment at the Montreal Neurological Institute.²¹ The residual subtraction artifacts from metal near the region of interest (ROI) are the most clinically relevant, and thus automated registration could be accelerated, and improved, using a smaller sub-section of the volume. Fortunately, patients are routinely anaesthetized during intervention, so patient motion would not be a problem in these studies. In this case, volumetric subtraction could be reliably performed without any re-registration of the mask volume. This is potentially important because of the time constraints imposed by the requirement of near real-time imaging during intervention.

Additional anatomical and functional information could be supplemented by fusing images that were previously acquired by other modalities. An excellent clinical application would be the treatment of arteriovenous malformations (AVMs). In this case, MRI and fMRI could be integrated and displayed during surgery, providing detailed knowledge of the AVM.^{22,23,24} This approach could reduce morbidity associated with surgical resection of normal brain tissue, which is estimated to be a complication in about 17% of AVM surgeries.²⁵

5. CONCLUSIONS

Using a prototype CRA system, we have performed volumetric subtraction angiography (VSA) on unanaesthetized patients. We have demonstrated sub-voxel registration of the anatomical mask and contrast-enhanced volumes. The resulting VSAs have provided unrivaled images of the clinically relevant vasculature near radiographically dense objects. Since the angiogram is not obscured by the dense objects, the VSAs provide superior visualization of the parent vessel and residual aneurysm near clips and coils. This illustrates the potential of this technique in both surgical and endovascular image-guided procedures. In addition, we believe that information from complementary imaging modalities (acquired pre-operatively), could be fused with the 3-D angiogram, thereby improving the efficacy of image-guided techniques such as the surgical resection of AVMs.

ACKNOWLEDGEMENTS

The financial assistance of Siemens Medical Systems (Erlangen), the Canadian Institutes of Health Research (grant No. MT-13356) and the Premier's Research Excellence Award is gratefully acknowledged; salary support was provided by the Heart and Stroke Foundation in the form of a Research Scholarship (DWH). We also thank B. Lehrbass, E. Rasimus, H. Nikolov, C. Norley, B. Kalamusky, G. Cowburn, J. Dix, S. Eggett, Dr. R. Fahrig, Dr. D. Pelz, and Dr. D. Lee for their contributions to this project.

REFERENCES

1. Guglielmi G, Vinuela F, Sepetka I, Macellari V. Electrothrombosis of saccular aneurysms via endovascular approach. Part 1: Electrochemical basis, technique, and experimental results. *Journal of Neurosurgery* 75;1-7 (1991).
2. Guglielmi G, Vinuela F, Dion J, Duckwiler G. Electrothrombosis of saccular aneurysms via endovascular approach. Part 2: Preliminary clinical experience. *Journal of Neurosurgery* 75;8-14 (1991).
3. Ebina K, Shimizu T, Sohma M, Iwabuchi T. Clinico-statistical study on morphological risk factors of middle cerebral artery aneurysms. *Acta Neurochirurgica* 106;153-159 (1990).
4. Richling B, Bavinzski G, Gross C, Gruber A, Killer M. Early clinical outcome of patients with ruptured cerebral aneurysms treated by endovascular (GDC) or microsurgical techniques. *Interventional Neuroradiology* 1;19-27 (1995).
5. Fernandez Zubillaga A, Guglielmi G, Vinuela F, Duckwiler GR. Endovascular occlusion of intracranial aneurysms with electrically detachable coils: correlation of aneurysm neck size and treatment. *AJNR* 15;815-820 (1994).
6. Mistretta CA. Relative characteristics of MR angiography and competing vascular imaging modalities. *Journal of Magnetic Resonance Imaging* 3;685-698 (1993).
7. Lin T, Fox AJ, Drake CG. Regrowth of aneurysm sacs from residual neck following aneurysm clipping. *Journal of Neurosurgery* 70;556-560 (1989).
8. Banerjee RK, Gonzalez CF, Cho YI, Picard L. Hemodynamic changes in recurrent intracranial terminal aneurysm after endovascular treatment. *Academic Radiology* 3;202-211 (1996).
9. Piotin M, Mandai S, Murphy K, et al. Dense packing of cerebral aneurysms: an in vitro study with detachable platinum coils. *AJNR* 21;757-760 (2000).
10. Tan CB, Kwok JCK, IU PP, Chan KY, Lam HS. The Feasibility of Three-Dimensional Guglielmi Detachable Coil for Embolisation of Wide Neck Cerebral Aneurysms. *Intervent Neurorad* 6:53-57, 2000.
11. Fillinger MF. New imaging techniques in endovascular surgery. *Surgical Clinics of North America* 79;451-475 (1999).
12. Payner TD, Horner TG, Leipzig TJ, Scott JA, Gilmor RL, DeNardo AJ. Role of intraoperative angiography in the surgical treatment of cerebral aneurysms. *Journal of Neurosurgery* 88;441-448 (1998).
13. Payner TD, Horner TG, Leipzig TJ, Scott JA, Gilmor RL, DeNardo AJ. Role of intraoperative angiography in the surgical treatment of cerebral aneurysms. *Journal of Neurosurgery* 88;441-448 (1998).
14. Origitano TC, Schwartz K, Anderson D, Azar-Kia B, Reichman OH. Optimal clip application and intraoperative angiography for intracranial aneurysms. *Surgical Neurology* 51;117-124 (1999).
15. Miyamoto S, Nagata I, Yamada K, et al. Delayed thrombus propagation after parent artery clipping for giant fusiform aneurysms of the circle of Willis. *Surgical Neurology* 51;89-93 (1999).
16. Bamford J, Sandercock P, Dennis M, Burn J, Warlow C. Classification and natural history of clinically identifiable subtypes of cerebral infarction. *Lancet* 337;1521-1526 (1991).
17. Fahrig R, Fox AJ, Lownie S, Holdsworth DW. Use of a C-arm system to generate true three-dimensional computed rotational angiograms: preliminary in vitro and in vivo results. *Ajnr: American Journal of Neuroradiology* 18;1507-1514 (1997).
18. Fahrig R, Moreau M, Holdsworth DW. Three-dimensional computed tomographic reconstruction using a C-arm mounted XRII: correction of image intensifier distortion. *Medical Physics* 24;1097-1106 (1997).
19. Fahrig R, Holdsworth DW. Three-dimensional computed tomographic reconstruction using a C-arm mounted XRII: Image-based correction of gantry motion non-idealities. *Medical Physics* 27;30-38 (2000).
20. Glover GH, Pelc NJ. Nonlinear partial volume artifacts in x-ray computed tomography. *Medical Physics* 3;238-248 (1980).
21. Neelin P, MacDonald D, Collins DL, Evans AC. The MINC file format: from bytes to brains. *Neuroimage* 7;786 (1998).
22. Zamorano L, Matter A, Saenz A, Portillo G, Diaz F. Interactive image-guided surgical resection of intracranial arteriovenous malformations. *Comput Aided Surg.* 1998; 3(2):57-63.
23. Schlosser MJ, McCarthy G, Fulbright RK, Gore JC, Awad IA. Cerebral vascular malformations adjacent to sensorimotor and visual cortex. Functional magnetic resonance imaging studies before and after therapeutic intervention.
24. Maldjian J, Atlas SW, Howard RS 2nd, Greenstein E, Alsop D, Detre JA, Listerud J, D'Esposito M, Flamm ES. Functional magnetic resonance imaging of regional brain activity in patients with intracerebral arteriovenous malformations before surgical or endovascular therapy. *J Neurosurg.* 1996 Mar;84(3):477-83.
25. Deruty R, Pelissou-Guyotat I, Amat D, Mottolese C, Bascoulergue Y, Gerard JP. Complications after multidisciplinary treatment of cerebral arteriovenous malformations. *Acta Neurochirurgica* 138;119-131 (1996).